ADL.

SCTB5

FIFTH STANDING COMMITTEE ON TUNA AND BILLFISH

18–19 June 1992
Honolulu, Hawaii

WORKING PAPER 7

(P. Kleiber and J. Hampton)

PROGRESS REPORT ON THE DEVELOPMENT OF THE SOLOMON ISLANDS FAD MODEL

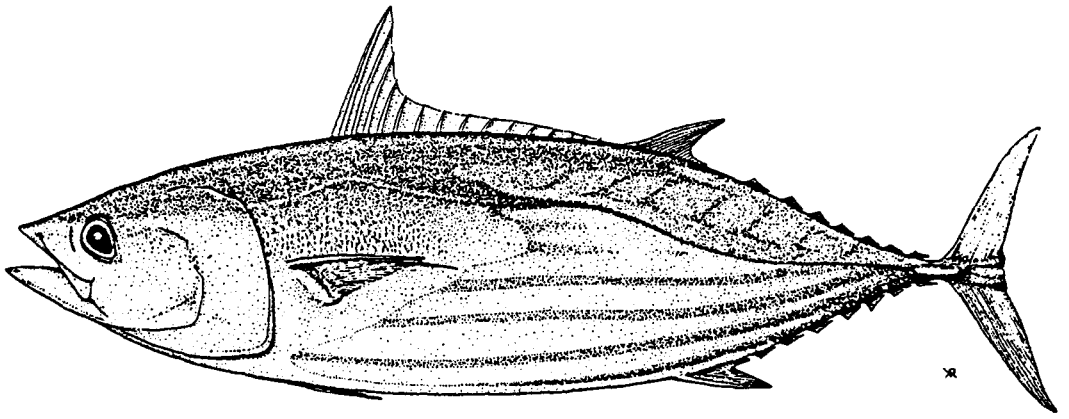

Tuna and Billfish Assessment Programme
South Pacific Commission
June 1992

Progress Report on the Development of the Solomon Islands FAD Model

P. Kleiber, and J. Hampton

Tuna and Billfish Assessment Programme
Noumea, New Caledonia

1. Introduction

The Solomon Islands, consisting of a main group archipelago (MGA) and several outlying islands or atolls (Figure 1), is the location of the largest locally-based tuna fishery in the Pacific Islands region. In recent years, the fishery has produced 30,000-40,000 t of tuna, the majority of which is skipjack (*Katsuwonus pelamis*).

Two main fishing techniques are employed, pole-and-line and purse seine. The pole-and-line fleet, consisting of thirty 59-GRT Japanese-type vessels, has unrestricted access throughout the Solomon Islands Exclusive Economic Zone (EEZ) outside of three miles from land, but most vessels usually fish within, or just outside, the MGA baseline (Figure 2), where they are in close proximity to productive baiting grounds. The purse seine fleet, consisting of one single seiner and three group seiners, is excluded from waters within the MGA baseline, and bases its operations around setting on fish aggregation devices (FADs) moored just outside the MGA baseline (Figure 3). Pole-and line vessels may also fish on these FADs and on others that are moored inside the MGA baseline, but their operations are much less FAD-dependent than those of the purse seiners.

To date, the pole-and-line fleet has produced in excess of 80% of the annual Solomon Islands skipjack catch (Table 1). However, purse seine catch rates, which averaged 27 t of skipjack per day in 1991 (SPC 1992) are much higher than those of pole-and-line vessels (5 t of skipjack per day in 1991). Also, the purse seiners catch substantial quantities of yellowfin (13 t per day in 1991), which are not generally taken in significant quantities by the pole-and-line fleet. On the basis of these catch rates, there is a strong economic incentive to expand purse seining. However, the Solomon Islands Government is concerned that a major increase in purse seine catch may negatively impact catch rates, and profitability, of the pole-and-line fleet, which although less efficient economically, is a major source of youth employment in the Solomon Islands and provides a superior product for the local cannery. In addition to this fishery interaction question, the overall potential of the skipjack fishery, while clearly substantial (Argue and Kearney 1982), has not yet been determined with precision.

To address these questions, the South Pacific Commission and the Solomon Islands Ministry of Natural Resources undertook a tagging programme in the Solomon Islands during 1989-1990. Six tagging cruises were undertaken over a 12 month period, releasing 7,730 tagged skipjack. From these releases, 914 recoveries have been recorded. The

experimental design of the tag release programme called for tagged skipjack, of the size range normally found in commercial catches (40-60 cm fork length), to be released throughout the major area of operation of the fishery. In particular, tagged skipjack were to be released both in areas fished by purse seiners (in the vicinity of FADs) and in areas fished by pole-and-liners (mainly within the MGA baseline). Four cruises were undertaken on pole-and-line vessels that were fishing commercially, therefore most releases were made to the south of New Georgia Island, which was the most productive fishing ground during these cruises (Figure 4). Two additional cruises were undertaken, using a chartered tagging research vessel, in order to release tagged skipjack in as many spatial strata as possible.

The principal questions to be posed in analysing the results of this tagging programme are:

1. What is the effect of the current purse seine fishery on the pole-and-line fishery?

2. What would be the effect of increased purse seine catches of skipjack on pole-and-line catch rates?

3. To what extent would further deployment of FADs enhance the operation of the fishery, and is it possible to recommend any particular spatial configuration of FADs that is likely to be more efficient?

4. Can a biologically reasonable development target, in terms of total catch, for the Solomon Islands skipjack fishery be defined, and if so, what is it?

In attempting to answer these questions, we developed a population dynamics model to describe skipjack natural death, harvest and movement, and have conducted some fits of the model to a subset of the tagging data. The model, described in detail below, explicitly incorporates the effects of FADs on skipjack movement. This spatial structure was a necessary inclusion to the model because it was clear from preliminary analyses (SPC, 1990) that the locations of tag releases in relation to the locations of the FADs was a key determinant in the pattern of tag recoveries by gear type. The objectives of this report are to provide a detailed account of the theory and methods used in implementing this model, to give preliminary results of fitting the model to the tagging data and to outline a strategy for using the model to answer the four questions posed above.

2. Description of Model

2.1 Basic Structure

The model deals with three basic processes: natural death, harvest, and movement in two horizontal dimensions. Because it is designed for tagged fish, recruitment is not an issue. The model also does not need to deal with growth or age, because we assume that the fish do not change their characteristics of mortality, vulnerability to the fishery, or movement once they reach size or age of recruitment to the fishery.

Most of the complexity of the model resides in the way it deals with movement. It is an advection/diffusion model on a discrete spatial grid of half degree squares. Thus the grid spacing is approximately 30 nautical miles in both spatial dimensions. The geographic boundaries (any of Figures 1-4) are such that we have an 18×22 spatial grid, and the population of tagged fish at large is represented by a corresponding 18×22 matrix, $\mathbf{P}$. Time is discretized into one month intervals. The spacing of time and spatial intervals reflects the resolution of the available data, both for tag recovery times and positions and for distribution of fishing effort — both necessary inputs to the model.

The basic movement parameter is diffusivity, D, which is translated into two transfer coefficients for each grid cell boundary, one in each direction. This means that there are four matrices of movement coefficients, $\mathbf{m}^{\uparrow}$, $\mathbf{m}^{\downarrow}$, $\mathbf{m}^{\rightarrow}$, $\mathbf{m}^{\leftarrow}$ which govern movement in north, south, east, and west directions respectively. The relationship of elements of the population matrix and the movement coefficient matrices to grid cells is organized as follows:

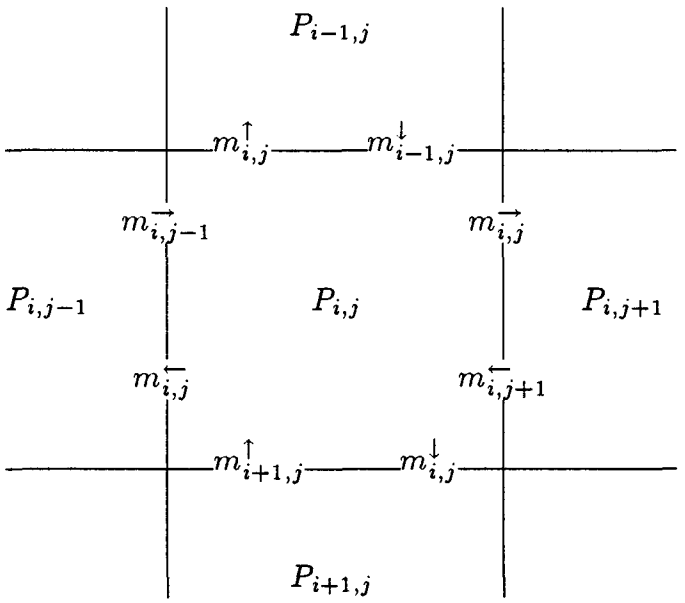

The movement coefficients are the proportion of the fish in one cell that move to a neighboring cell per unit time. For example, the instantaneous rate of movement from cell (i,j) to $(i,j+1)$ would be given by $m^{\rightarrow}_{i,j}P_{i,j}$.

Adding up the effects of movement, and mortality, the difference equation for projecting the population of tagged fish in cell (i,j) at time t by one time step, Δt, is given by

$$\begin{aligned} P_{i,j,t+\Delta t} = P_{i,j,t} + \\ \Delta t \Big[& m^{\uparrow}_{i+1,j} P_{i+1,j,t} + m^{\downarrow}_{i-1,j} P_{i-1,j,t} + m^{\rightarrow}_{i,j-1} P_{i,j-1,t} + m^{\leftarrow}_{i,j+1} P_{i,j+1,t} \\ & - \Big(m^{\uparrow}_{i,j} + m^{\downarrow}_{i,j} + m^{\rightarrow}_{i,j} + m^{\leftarrow}_{i,j} + M + \sum_k q_k e_{i,j,k,t} \Big) P_{i,j,t} \Big] \end{aligned} \tag{1}$$

where M in the natural mortality, q_k is the catchability for the k-th gear-type, and $e_{i,j,k,t}$ is the corresponding effort of gear k in the cell at time t. We have two gear types in the present implementation of the model, purse-seine and pole-and-line. These account for almost all ($> 99\%$) of the tag returns.

The edges of the grid must be handled specially. In this model, we have closed borders, which means that no fish can migrate into or out of our model area. In effect, the movement coefficients of the outer boundary are defined to be zero, that is, for our 18 by 22 grid:

$$\begin{aligned} m^{\uparrow}_{1,j},\ m^{\downarrow}_{0,j},\ m^{\uparrow}_{19,j},\ m^{\downarrow}_{18,j} \equiv 0 \quad \forall\ j \\ m^{\leftarrow}_{i,1},\ m^{\rightarrow}_{i,0},\ m^{\leftarrow}_{i,23},\ m^{\rightarrow}_{i,22} \equiv 0 \quad \forall\ i \end{aligned} \tag{2}$$

However, we have a trick for effectively opening the borders by setting the surface area of the edge cells to artificially high values (see next section).

2.2 Determining Movement Coefficients

In the absence of local conditions that would modify movement behavior, it is assumed that movement would be purely diffusive. In this case all movement coefficients in the model would be assigned a common value, which would be a diffusion coefficient, D. However, the presence of FADs or islands modifies the values that are assigned to local movement coefficients as follows:

$$\begin{aligned} m^{\uparrow}_{i,j} &= D \cdot \phi_{i,j} b^p_{i-1,j} / a_{i,j} \\ m^{\downarrow}_{i,j} &= D \cdot \phi_{i,j} b^p_{i,j} / a_{i,j} \\ m^{\rightarrow}_{i,j} &= D \cdot \phi_{i,j} b^m_{i,j} / a_{i,j} \\ m^{\leftarrow}_{i,j} &= D \cdot \phi_{i,j} b^m_{i,j-1} / a_{i,j} \end{aligned}$$

where ϕ, b^p, b^m, and a are elements of matrix, $\mathbf{\Phi}$, describing effects of FADs, and matrices, $\mathbf{b}^p$, $\mathbf{b}^m$, and $\mathbf{a}$, describing various effects of islands.

a. Effect of FADs

The effect of FADs is, of course, the central thrust of the model. Other than the well known and well utilized observation that tuna congregate in the neighborhood of FADs,

little is known about how FADs might modify movement behavior. Observations of course tracks of individual tunas (Holland et al., 1990) in some cases show obvious attraction to FADs, but it is not obvious how to translate these observations into numerical parameters of movement. In our model, we have assumed that FADs in a grid cell inhibit the movement of fish out of that cell. This is accomplished by reducing the exit coefficients of cells by factors which are the corresponding elements of Φ, given by

$$\phi_{i,j} = 1 - \frac{s f_{i,j}}{f_h + f_{i,j}}; \quad 0 \leq s \leq 1, f_h \geq 0. \tag{3}$$

where $f_{i,j}$ is the number of FADs in cell (i,j). The theoretical justification for Equation 3 lies not in its particular mathematical form, but in the fact that it behaves as we would expect. Thus in cells with no FADS there is no effect ($\phi = 1$), and with increasing number of FADs, the effect increases (ϕ decreases) and approaches a saturation level ($\phi \rightarrow 1-s$) for cells with a large number of FADs. The parameter, f_h, is the number of FADs in a cell that gives half the saturation effect.

b. Effect of Obstruction by Islands

The other condition that modifies movement coefficients is the presence of islands. There are two effects. One is the obstruction of boundaries between cells, and the other the obstruction of water area within cells. To prevent the situation of cells being cut into two isolated parts, we shifted some of the islands slightly (in the model!), the data resolution being insufficient to assign effort and tag returns to sub-areas within cells. In these cases, we guessed which side of the island most of the data originated from and shifted the island so that all the water area in the cell was on that side. We estimated the proportion of each boundary and the proportion of the area of each cell that is open (i.e, *not* obscured by islands). These data make up three matrices, $\mathbf{a}$, the proportion of water area in cells, $\mathbf{b}^m$, the proportion of each meridional (longitudinal) boundary open for east-west movement, and $\mathbf{b}^p$, the proportion of each parallel (latitudinal) boundary open for north-south movement. The indexing of elements of these matrices in relation to the grid cells is as follows:

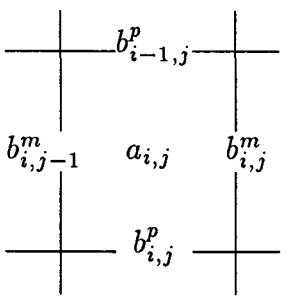

The trick alluded to above for opening the borders of the model area involves setting the edge elements of $\mathbf{a}$ (i.e., $a_{1,.}$, $a_{18,.}$, $a_{.,1}$, $a_{.,22}$) to values much greater than unity (normally these numbers are proportions, ie., between 0 and 1). This has the effect of making the edge cells into population sinks because their surface areas are in effect much larger than the interior cells.

The obscuring of area in cells by islands has an additional effect, not on movement, but on fishing mortality. A given amount of effort is more effective if the fish and the gear are crowded into a smaller area. In the model, we handle this by modifying (enhancing) the effort by the reciprocal of the area factor, that is,

$$e_{i,j,k,t} = e^{o}_{i,j,k,t}/a_{i,j} \quad \forall \; i,j,k,t$$

where $e^{o}_{i,j,k,t}$ is the raw effort.

2.3 Simulation Method

To run the model we generate a solution over time to Equation 1 for each tag set and for all cells in the grid starting from known initial conditions (given by tag release information). We defined a tag set as the releases within a calendar month and within one half-degree cell. The number released is multiplied by an initial tag survival factor to get the effective number of releases. This factor includes the effect of non-reporting as well as immediate tagging mortality and tag shedding. To generated a solution, we use an alternating direction implicit method (Press, et al. 1988, pg 666). This is essentially the same method developed by Sibert and Fournier (pers. comm.) for a large scale tuna movement model. It enables us to get stable solutions with rather large diffusion turnover of several hundred percent per time step in the grid cells.

2.4 Method for Fitting Model to Data

We use a strategy similar to that of Hilborn (1990), Deriso et al. (1991) and Sibert and Fournier (pers. comm.) to fit the model to tag data. In our case, we maximize a likelihood function which is the probability of observing what we did observe (the real data), under the assumption that the returns predicted from the model are the real expected values for the returns. Under that assumption, the probability of any one tag being returned from a particular time-area stratum is the predicted number of returns in that stratum divided by the effective number of releases in the particular tag set, and the probability of not being returned is the predicted number of non-returns divided by that same number of releases. Combining the probabilities of all the actual tag returns as well as the probabilities for all the tags that were not returned, the likelihood of the observed data, $\mathbf{r}$, given the predicted data, $\mathbf{p}$, is the following product of multinomial functions:

$$\mathcal{L}(\mathbf{r}|\mathbf{p}) = \prod_{s}\Big[\frac{R_s!}{(\prod_i r_{i,s}!)(R_s - \sum_i r_{i,s})!}\Big(1 - \frac{\sum_i p_{i,s}}{R_s}\Big)^{\left(R_s - \sum_i r_{i,s}\right)} \prod_{i}\Big(\frac{p_{i,s}}{R_s}\Big)^{r_{i,s}}\Big] \quad (7)$$

where

R_s = effective number of releases in tag set s

$r_{i,s}$ = observed tag returns in stratum, i and tag set, s

$p_{i,s}$ = predicted tag returns in stratum, i and tag set, s

Since the predicted returns, $\mathbf{p}$, depend on the parameter values that go into the model, we can search for the set of parameter values that maximize the likelihood function. Actually, we find the minimum of the negative log of the likelihood function, which amounts to the same thing. We make use of programming package, AUTODIF, which is designed for non-linear function minimization using an iterative quasi-Newton routine and a built-in system for automatically finding the required partial derivatives of the function being minimized (Anonymous, 1991). In estimating six parameters consisting of diffusivity, two FAD stickiness parameters, natural mortality and two catchabilities, the fitting procedure tends to converge in 10 to 100 iterations depending on how close the original parameter guesses are to the final estimates. With simulated data sets the final estimates are close to the parameters used in the simulation to within four or five significant figures.

3. Preliminary Results and Discussion

So far we have fitted the model to the two tag sets (releases in one month and one cell) that had the highest number of releases, 1,938 and 1,817. The remaining sets range down from 637 to 1 release. We found that the model converged in almost all cases except where there were too few subiterations or some parameters were not constrained enough, resulting in negative populations in the model. Table 2 gives information on fits that did converge.

The model "wanted" to estimate a rather high diffusivity. In the first trial in Table 2, with only two subiterations per time step, the final diffusivity estimate was pushed against the upper constraint. To relax the constraint and let the fitting procedure find it's natural diffusivity level, we had to increase the number of subiterations to avoid negative populations in the model. With four subiterations, the final estimate stabilized at approximately 3 grid cell areas per month (2700 square nautical miles per month). This corresponds to a monthly turnover in a cell of several hundred percent per month due to diffusive movement. The reason for this high estimate is the fact that the model has to accommodate returns that were made from several cells away from the release cells within the first month or so.

Some of the trials were repeated with different starting values for the parameters or restarted at the final converged values. In most cases these repeat trials reconverged to essentially the same point, except for the trial with three subiterations, which wandered into negative population territory when it was restarted. That is why we advanced to four subiterations.

In moving up to four subiterations the measure of fit got worse rather than better. We are not sure why this is. The trial conditions listed in Table 2 are not the whole story because there was some fixing of bugs in the computer program between one trial and another. We think these were minor bugs, but they might have had subtle effects. This is a primary reason why the results presented here are preliminary. The differences among the last three trials, however, are strictly as listed in the table.

Estimation of the FAD stickiness parameters, s, and f_h, is the central thrust of this work. We hoped the model would be sensitive to those parameters, and it turns out that it is. Convergence was achieved in some cases with starting values of these parameters rather far from the final estimates — starting close to 0 or 1 for s or as high as 20 for f_h. Throughout the change in fitting conditions (Table 2) the FAD parameter estimates persisted with s roughly in the middle of its possible range (0-1) and with f_h between 1.3 and 1.9. Trial 7, which was identical with Trial 6 in every respect except that the FAD effect was disabled, gave a significantly worse fit.

$$\chi^2_{[2\,df]} = 2(604.49 - 595.66) = 17.66$$
$$\text{probability} = .00015$$

Thus it appears that there is some effect of FADs implicit in the data and that the model captures at least part of that effect. According to the estimated values of the FAD parameters, the tendency of skipjack to exit a cell can be reduced by more than half with five or six FADs in the cell, but the effect of adding more FADs than that is greatly diminished (Figure 5).

The remaining parameter estimates, natural mortality, and catchabilities, contain no surprises. Attrition rates as high or higher that the estimates of M in Table 2 are routinely found for skipjack from simpler models lacking fish movement. Our estimates are within the confidence range of attrition estimates for skipjack in the Solomon Islands reported by Argue and Kearney (1982). As expected, the catchability estimates for purse seine are higher than for pole-and-line. The catchability for pole-and-line is much higher than reported by Argue and Kearney (1982), but that is also expected because their catchabilities apply to the whole stock of the fishery whereas ours apply only to the population in a half-degree cell.

To further evaluate our parameter estimates, it would be nice to estimate confidence limits. The best way to do that would be a Monte-Carlo type exercise, requiring hundreds of fitting trials to stochastically generated data sets. We did generate 200 data sets using the multinomial probabilities (same as in Equation 7) from the best fitting outcome of the model (Trial #6, Table 2). To fit the model to all those data sets is unfeasable at the moment because each fitting run requires up to 10 hours to converge on parameter estimates. However, there is hope for considerable improvement in the efficiency of the fitting procedure. In the meantime, we have used the Monte-Carlo data sets in other ways (see below).

To evaluate the performance of the model by comparing real and predicted tag returns is difficult because of the multidimensional nature of the data (tag set, gear type, month, location north/south, location east/west). Therefore we did a couple of comparisons between aggregates of data predicted by the model against aggregates of data used to fit the model. Figure 6 is the overall tag return rate with time at large, and Figure 7 is the mean distance from cell of release with time. The confidence bands were obtained by calculating 200 aggregate tag returns (Figure 6) or mean distance

(Figure 7) in each months-at-large category using the 200 Monte-Carlo data sets. We then took the 2.5% and 97.5% quantiles from each months-at-large category.

In Figure 6, if we imagine that the confidence bounds were not there, it would appear that the model fit is best in the early months and deteriorates after about 10 months at large. There is a natural tendency for this to be so in this type of logarithmic attrition plot. The model can legitimately predict fractional returns — even less than one return, but fractional returns cannot happen in reality, nor can zero returns be represented on the logarithmic plot. The effect is that the points tend to be far from the predicted line. This effect is accounted for in the confidence bounds, which broaden with time at large, and we can see that the worst fit of the model according to Figure 6 is actually in the first three months. Note, however, that the deviations between observed and predicted values in this figure (and also in Figure 7) do not explicitly enter into the fitting process. It is the observed and predicted returns in individual spatio-temporal strata that go into the likelihood function. The confidence bounds in Figure 7 also broaden with time at large because of diminishing number of predicted tag returns. The worst fit in this case is in the first month where the actual mean distance of recovery was greater than predicted.

Compared to the way most fishery models fit their data, the match between observed and predicted shown in Figures 6 and 7 seems pretty good. To further evaluate the model, we calculated negative log likelihoods for each of the Monte-Carlo data sets. We found that the negative log likelihood from the real data falls far outside the frequency distribution of such values from the Monte-Carlo data (Figure 8), which means that the the model is failing in some detail or other that seems to give difficulties in the first few months, judging from Figures 6 and 7. This test of fit may be overly harsh because additional considerations could imply that the Monte-Carlo distribution should be broader, for example if the tagged fish were not fully independent of each other. Nevertheless, all models fail somewhere, and it is desirable to examine their failings to help interpret results and perhaps to suggest improvements.

To try to pinpoint further where the model deviates from the observed tag returns or possibly to find a pattern in its deviation, we calculated a deviance for each spatiotemporal stratum containing effort given by:

$$\mathcal{D}_{i,s} = -2\log\left[\left(\frac{p_{i,s}}{r_{i,s}}\right)^{r_{i,s}}\left(\frac{R_s - p_{i,s}}{R_s - r_{i,s}}\right)^{\left(R_s - r_{i,s}\right)}\right] \tag{8}$$

where i is the stratum, and s is the tag set. Like the familiar square of residuals, the deviances are always positive whether the observed value is greater than or less than the predicted value, and the larger differences are heavily emphasized. Again, multidimensionality is a problem in visualizing the results. Therefore we sorted the recovery strata into months-at-large by distance-from-release categories. Examining the maximum deviance in each category in which the model predicted fewer than the observed number of returns, we found that the largest of these deviances are concentrated one to four cells distant from the release cell and in the early months following the month of

release (Figure 9). On the other hand, by far the largest deviance in which the model predicted more than the observed number of returns was in the first month and the cell of release (Figure 10).

Part of the problem here may have to do with the fact that the model presumes all tags are released at the beginning of the first month in the middle of the release cell, whereas in fact, tags are released throughout the first month and throughout the cell and in some haphazard distribution in time and space. That there is any distribution at all of release times during the release month means that not all releases are exposed to effort for the whole month, which could explain the over-estimate of returns in the release cell and month (Figure 10). A non-ideal distribution of releases is a very common problem in models built for analyzing tag experiments. It is usually dealt with by ignoring the returns in the first one or two time periods. We have not tried that trick yet, bit it is on our list of things to do.

We suspect that there is another problem which we may be able to deal with by adjusting the model. It appears, particularly from Figure 9, that to improve the fit, the model must quickly move more tagged fish from release cells to nearby cells with effort within the first few months in order to realize the observed number of returns in those cells. The only way the model has to do this is to increase the diffusivity, but in doing so, the diffusive loss to the numerous cells without effort will be increased which would cause the attrition rate to be too high. It may be that the rate of movement of fish within and near the archipelago (where most of the effort is located) is indeed very high, but that there is a reluctance to leave the vicinity of the islands. We could model this effect by adding a diffusion barrier around the archipelago that would lower the chances of fish straying away even though they have a propensity for rapid movement within the archipelago. This is also on our list of things to try.

Lastly, other that using the model to address management questions (see next section), we hope to improve the efficiency of the fitting process to allow us to include more of the tag sets in the fitting process and to conduct Monte-Carlo type assessments of parameter confidence limits.

4. Strategy for Use of the Model to Address Management Questions

Ultimately, we wish to be able to use this model to answer the four questions posed earlier in the report. To do this, we first need to devise a means of applying the model parameter values that were estimated for tagged skipjack to the untagged skipjack population in general. The best way to do this may be to use a simulation approach similar to that of Kleiber and Baker (1987) based on a model much like equation 1 but with recruitment added in. In simple terms, the procedure would be as follows:

1. Determine a fishing pattern (catch and effort, by gear type, by spatial grid) from the available fishery data that is typical of current conditions in the fishery.

2. Establish the steady-state population conditions associated with this average fishing pattern, by allowing the model to proceed from reasonable starting conditions, distributing the population according to FAD, island and harvest effects until an equilibribum pattern is reached. It will be necessary to assume some reasonable pattern of recruitment to the fishery. The real recruitment pattern is of course unknown, but the effects of plausible alternative patterns could be investigated using the model. The scale of recruitment can be adjusted so that the catch in the model is roughly equivalent to the real average catch. Being in equilibrium, the model will be independent of the starting population; so we need not worry about precise estimation of starting population levels.

3. Having established equilibrium conditions, the system can then be perturbed by altering the fishing pattern and the response of the population observed.

Each of the four questions posed earlier might then be investigated as follows:

1. The effect of the current purse seine fishery on pole-and-line catch rates could be estimated by setting purse seine effort in all spatial grids to zero and maintaining the current pattern and level of pole-and-line effort. The difference between the original pole-and-line catch rates and their new equilibrium levels would be a measure of the effect of the current purse seine fishery on the pole-and-line fishery.

2. An identical analysis could be performed to determine the effect of specified increases in purse seine effort on pole-and-line catch rates.

3. Similarly, various new patterns of FAD deployment and numbers of FADs could be simulated, and the resulting effects on purse seine and pole-and-line catch rates observed.

4. Various trial combinations of increased purse seine and pole-and-line effort could be simulated and the resulting effects on aggregate equilibrium population size over the study area examined. Development options could then be assessed, based on some criterion as to what constitutes an acceptable reduction in equilibrium population.

5. References

Anonymous. 1991. AUTODIF: A C++ array language extension with automatic differentiation for use in nonlinear modeling and statistics. Otter Research Ltd., Box 265, Station A, Nanaimo B.C., Canada.

Argue, A., and R.E. Kearney. 1982. An assessment of the skipjack and baitfish resources of Solomon Islands. Skipjack Survey and Assessment Programme Final Country Report No. 3. South Pacific Commission, Noumea, New Caledonia. 73p.

Deriso. R.B., R.G. Punsly, and W.H. Bayliff. 1991. A markov movement model of yellowfin tuna in the eastern Pacific Ocean and some analyses for international management. Fisheries Research, 11:375-395.

Hilborn, R. 1990. Determination of fish movement patterns from tag recoveries using maximum likelihood estimators. Can. J. Fish. Aquat. Sci., 47:635-643.

Holland, K.N., R.W. Brill, and R.K.C. Chang. 1990. Horizontal and vertical movements of yellowfin and bigeye tuna associated with fish aggregating devices. Fish. Bull. (U.S.), 88:493-507.

Kleiber, P., and B. Baker. 1987. Assessment of interaction between north Pacific albacore, *Thunnus alalunga*, fisheries by use of a simulation model. Fish. Bull. U.S., 4:703-711.

Press, W.H., B.P. Flannery, S.A. Teukolsky, and W.T. Vetterling. 1988. Numerical Recipes in C. Cambridge University Press, NY. 735 p.

SPC. 1990. Preliminary analysis of Solomon Islands In-Country Tuna Tagging Project data. Third Standing Committee on Tuna and Billfish, (Noumea, New Caledonia, 6-8 June 1990), Working Paper 4. South Pacific Commission, Noumea, New Caledonia.

SPC. 1992. Regional Tuna Bulletin 4th Quarter 1991. South Pacific Commission, Noumea, New Caledonia. 41p.

Table 1. Effort (boat-days), catch (metric tonnes), and catch per unit effort for purse-seine and pole-and-line gear in the Solomon Islands.

Year	Purse-seine					Pole-and-line				
	Effort	Skipjack		Yellowfin		Effort	Skipjack		Yellowfin	
		Catch	CPUE	Catch	CPUE		Catch	CPUE	Catch	CPUE
81						4661	19541	4.19	209	.04
82						5008	16417	3.28	227	.05
83						5918	26912	4.55	575	.10
84	179	1982	11.1	1563	8.7	6269	29488	4.70	336	.05
85	87	1199	13.8	1236	14.2	7095	23680	3.34	337	.05
86	177	3044	17.2	2109	11.9	7488	36139	4.83	565	.08
87	189	3462	18.3	2959	15.7	6838	20556	3.01	1456	.21
88	231	3902	16.9	2832	12.3	7483	28613	3.82	1189	.16
89	317	5758	18.2	4198	13.2	6809	23187	3.41	774	.11
90	325	4037	12.4	3595	11.1	5837	17418	2.98	1100	.19
91	307	7674	25.0	3816	12.4	6829	35240	5.16	953	.14

Table 2. Results of fitting model to two tag sets (see text), giving the salient conditions of each fit, the parameter values to which the procedure converged, and the negative log likelihood measure of goodness of fit. Parameter units are: D (cell-area mo^{-}1), s (unitless), f_h (# FADs), M (mo^{-}1), q (cell-area boat-day^{-}1 mo^{-}1).

#	Conditions				Estimated Parameters						Goodness of Fit
	Subiterations	Border	Island Obst.	Init. Tag Survival	D	s	f_h	M	Seine q	P&L q	$-\log(\mathcal{L})$
1	2	closed	no	1.0	2.5*	.49	1.3	.14	.026	.00072	575.64
2	3	closed	no	1.0	3.4	.61	1.8	.13	.026	.00078	587.85
3	4	closed	no	1.0	3.1	.70	1.5	.13	.021	.00071	596.33
4	4	closed	no	.9	3.1	.70	1.5	.13	.023	.00079	597.05
5	4	closed	yes	.9	3.1	.75	1.9	.13	.021	.00072	596.05
6	4	open	yes	.9	3.2	.69	1.5	.12	.023	.00079	595.66
7	4	open	yes	.9	2.7	—†	—†	.11	.037	.00089	604.49

* Converged on upper constraint.
† FAD effect disabled.

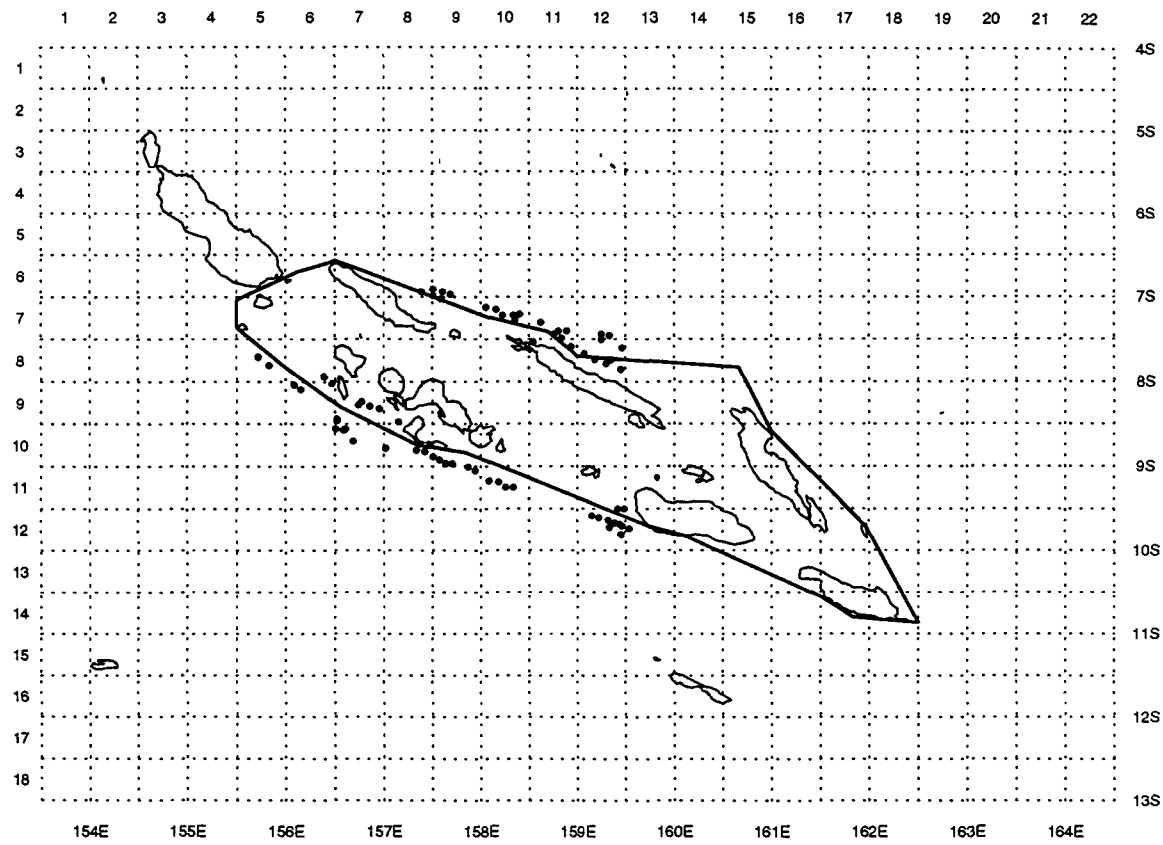

Figure 1. Study area showing the Solomon Islands main group archipelago baseline (heavy line) and the location of FADs (solid circles).

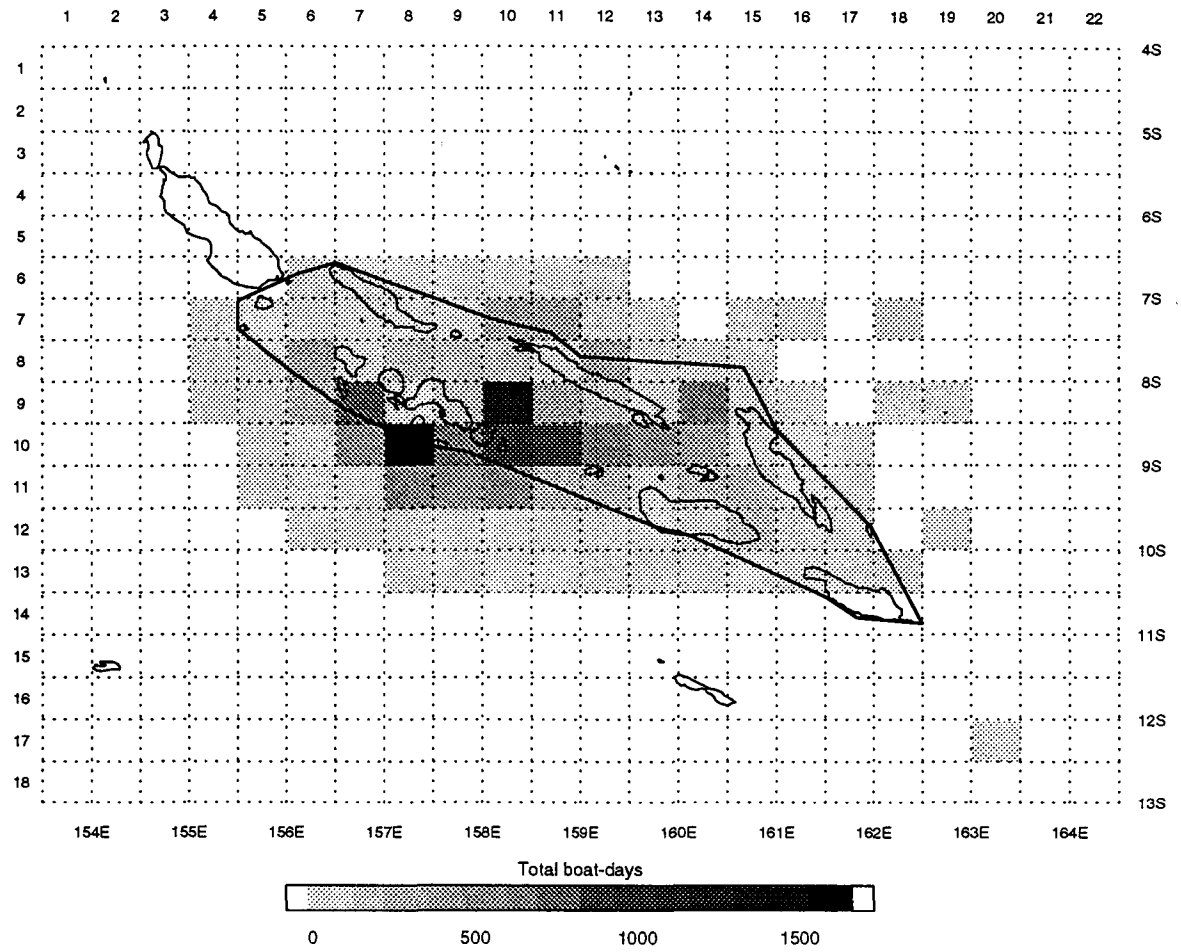

Figure 2. Aggregate distribution of pole-and-line effort in the study area from mid-1989 through 1991.

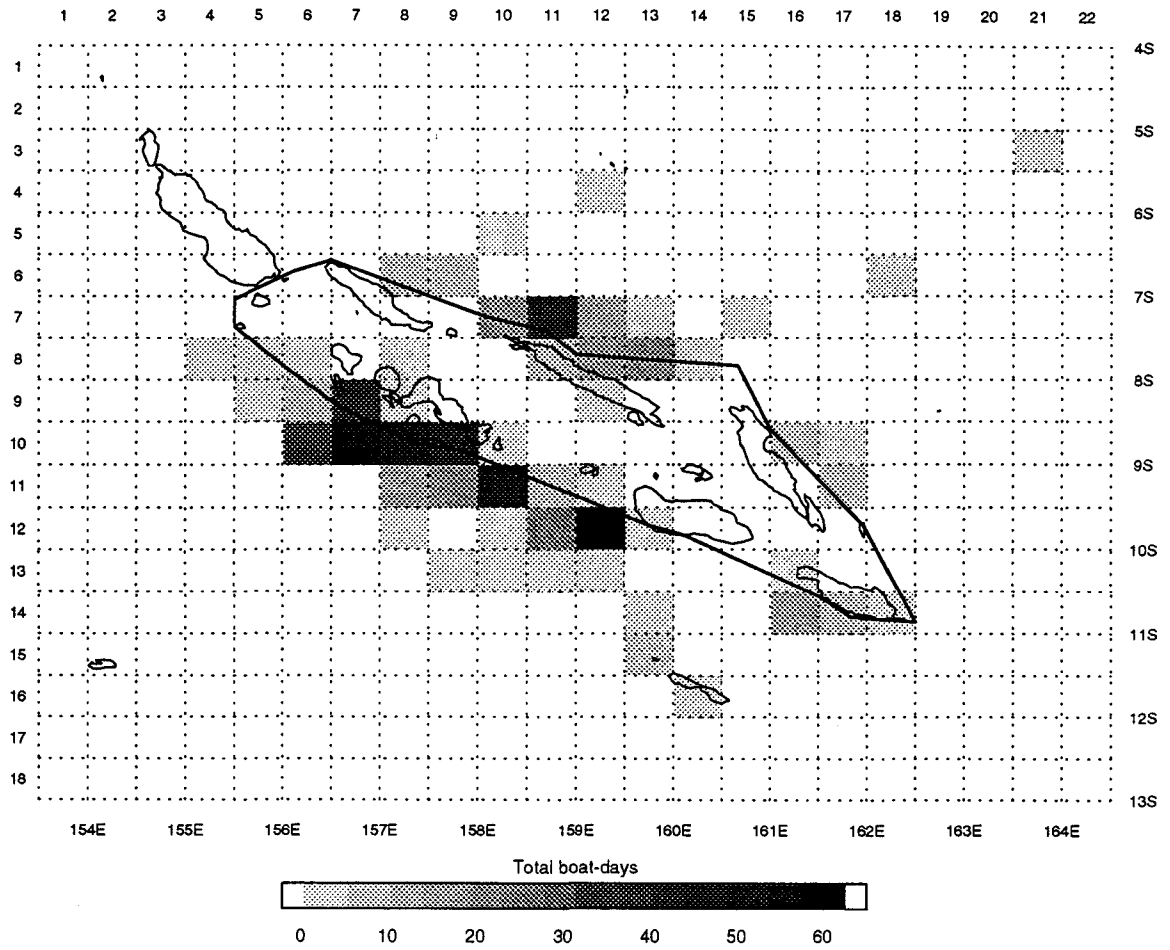

Figure 3. Aggregate distribution of purse-seine effort in the study area from mid-1989 through 1991.

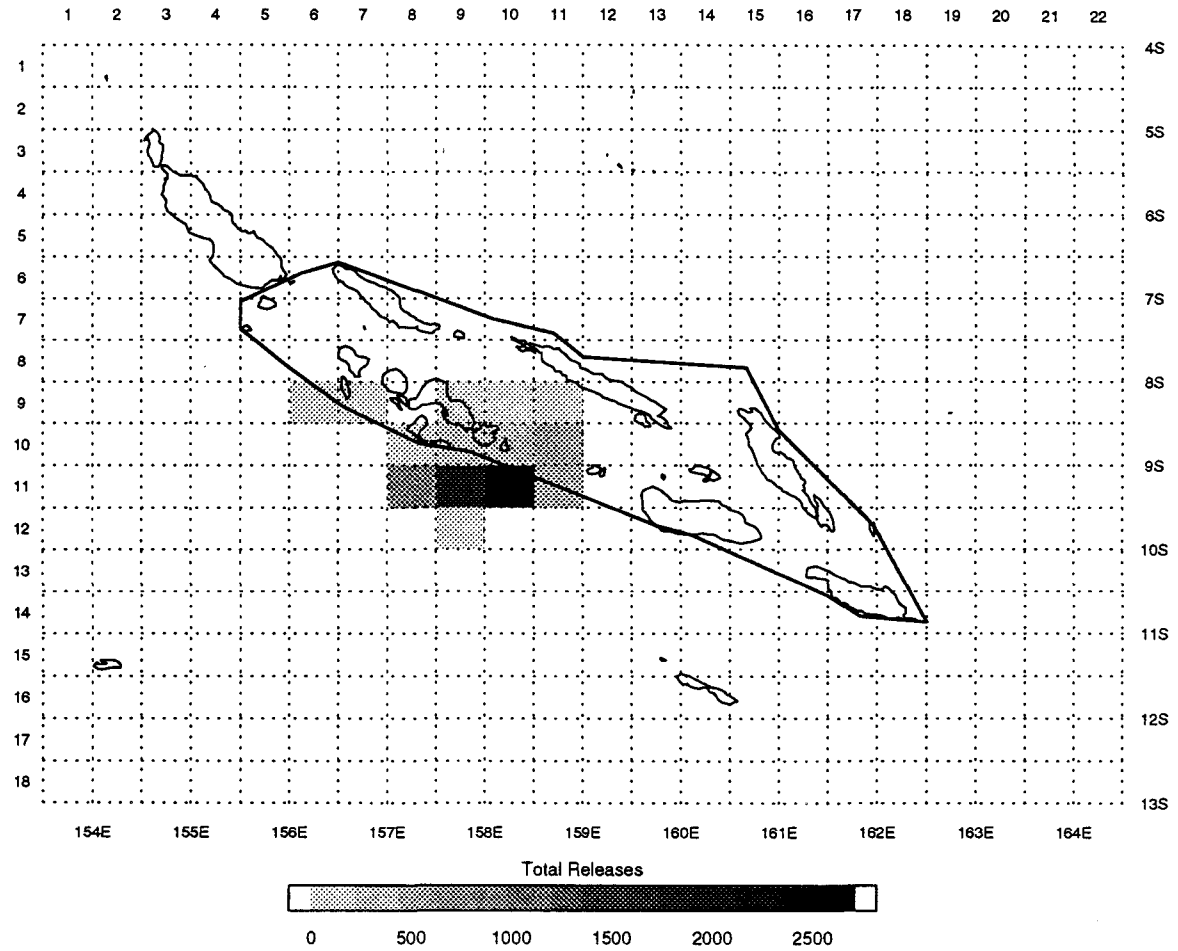

J.C.

Figure 4. Distribution of tag releases in Solomon Islands, 1989-1990.

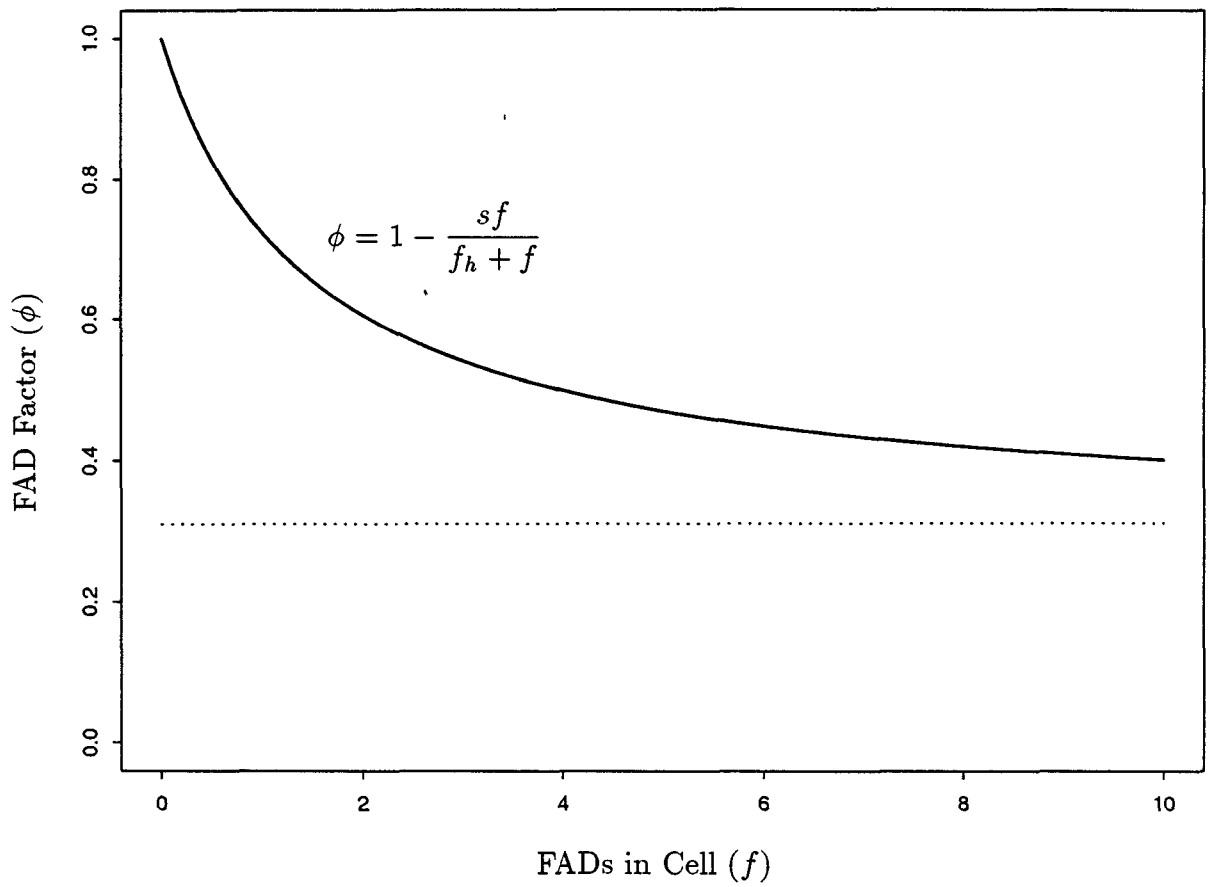

Figure 5. FAD effect as function of number of FADs in a cell for FAD parameters from the best fitting trial (#6 in Table 2). Dotted line is saturation effect of FADs.

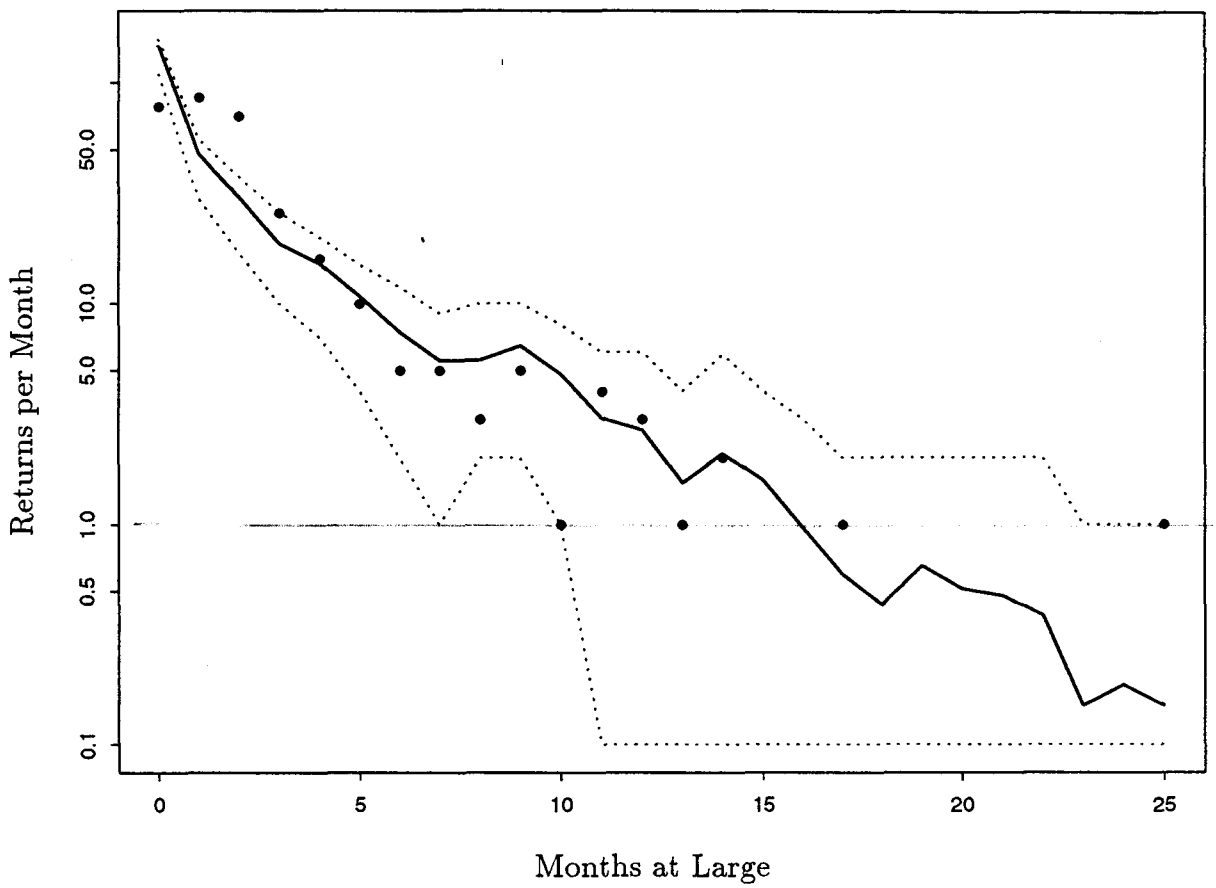

Figure 6. Aggregate tag attrition. Solid line is expected aggregate returns per month predicted by the model with best fitting parameters. Points are the observed aggregate returns for the two tag sets used in fitting the model. Dotted lines are 95% Monte-Carlo confidence bounds (see text). The lowest levels of the lower confidence bounds are actually zero.

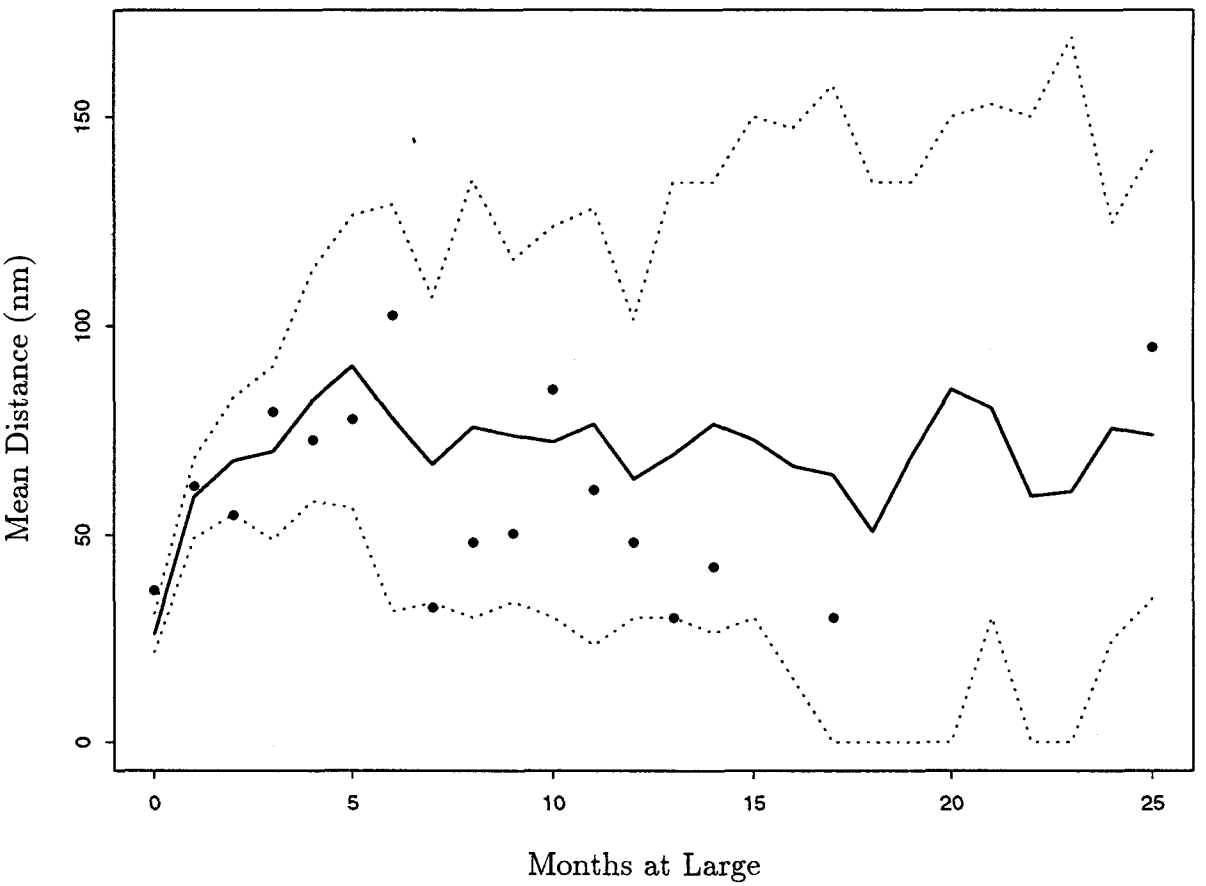

Figure 7. Mean distance with time. Solid line is mean distance of recoveries from release point predicted by mode with best fitting parameters. Points are the observed mean distance of recoveries for the two tags sets used in fitting the model. Dotted lines are 95% Monte-Carlo confidence bounds (see text).

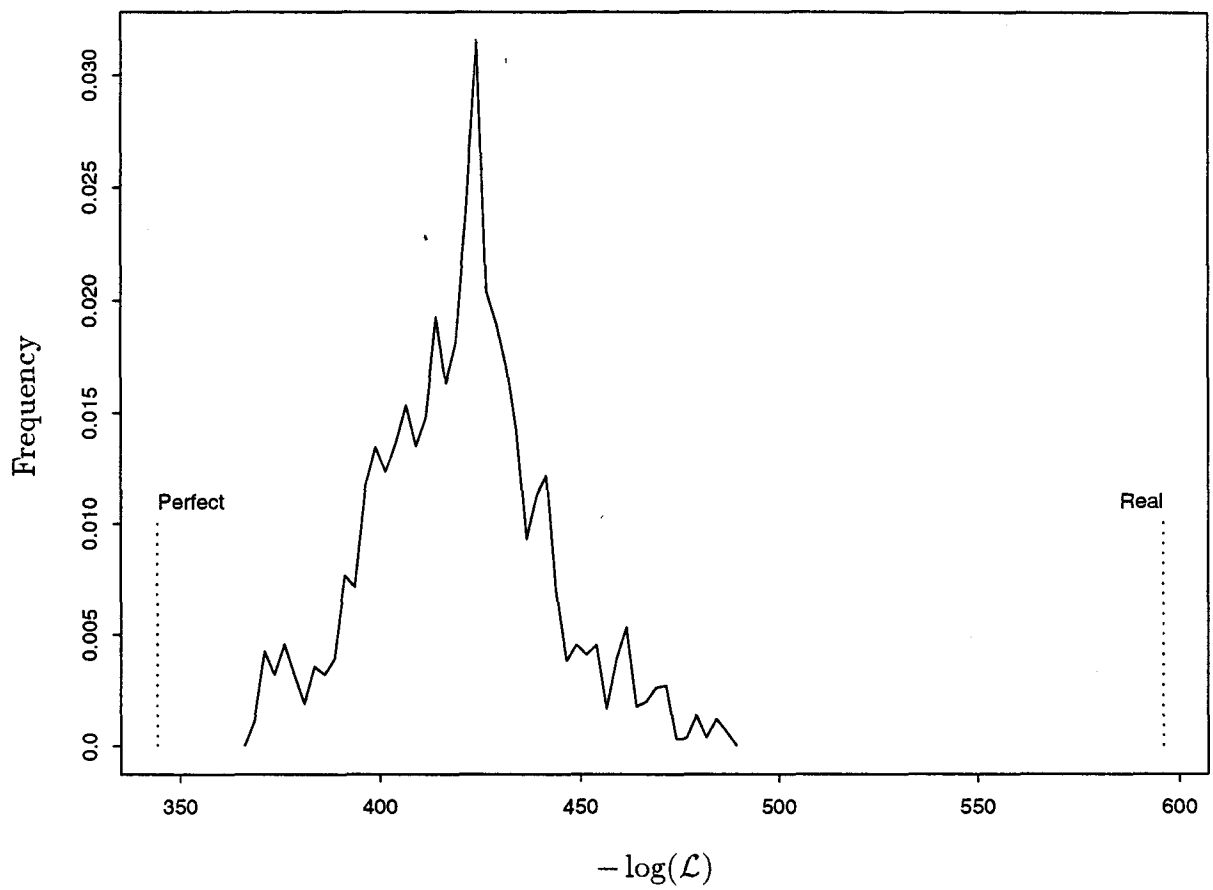

Figure 8. Monte-Carlo distribution of negative log likelihoods (see text). The level marked "perfect" is negative log likelihood for a hypothetical, and impossible, data set identical to the best fitting outcome of the model — impossible because it contains fractional returns. The level marked "real" is the negative log likelihood for the real tag return data.

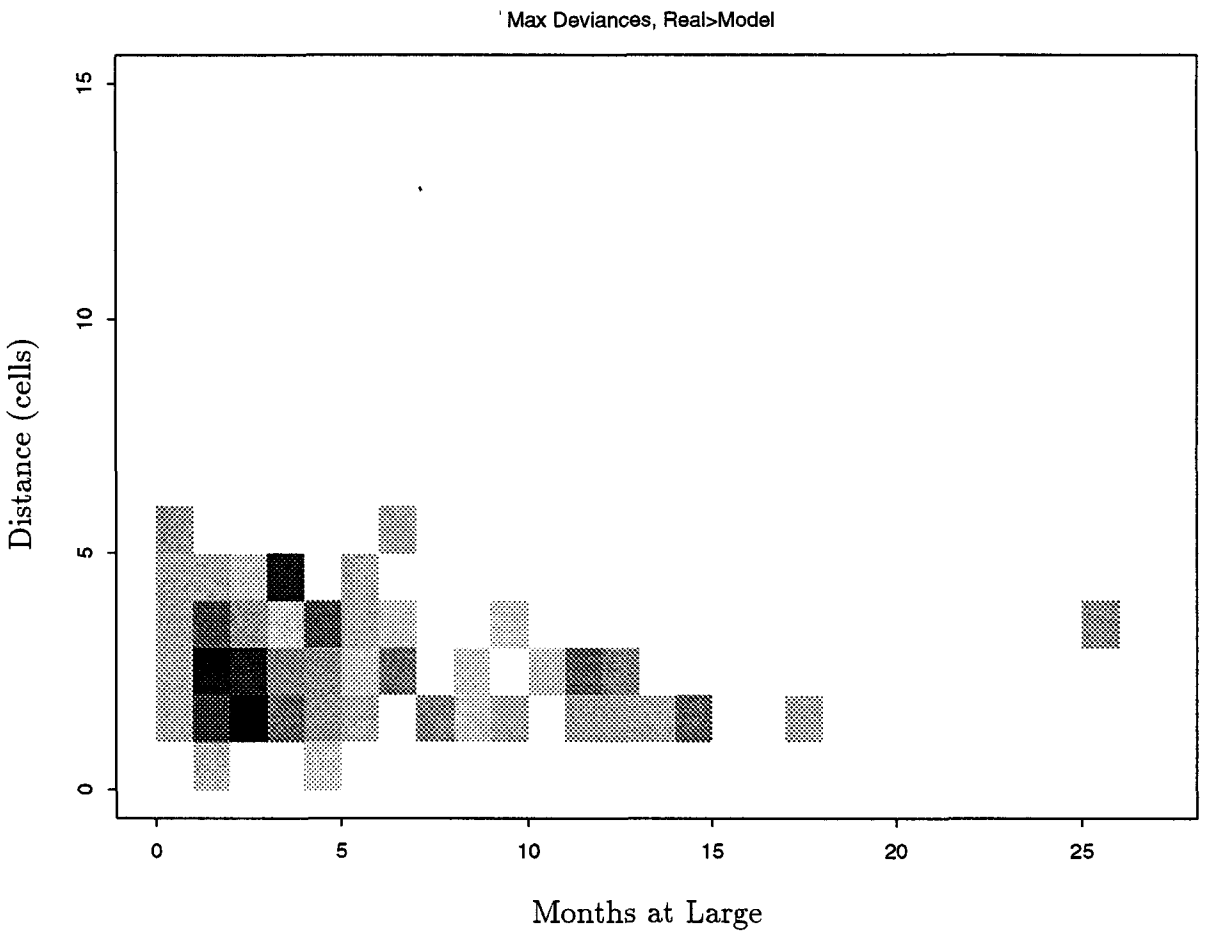

Figure 9. Maxima of deviances in categories of distance from cell of release (measured in cell widths of 30 nm) and months at large, and for spatiotemporal strata in which the best fitting outcome of the model predicts fewer than the real number of returns.

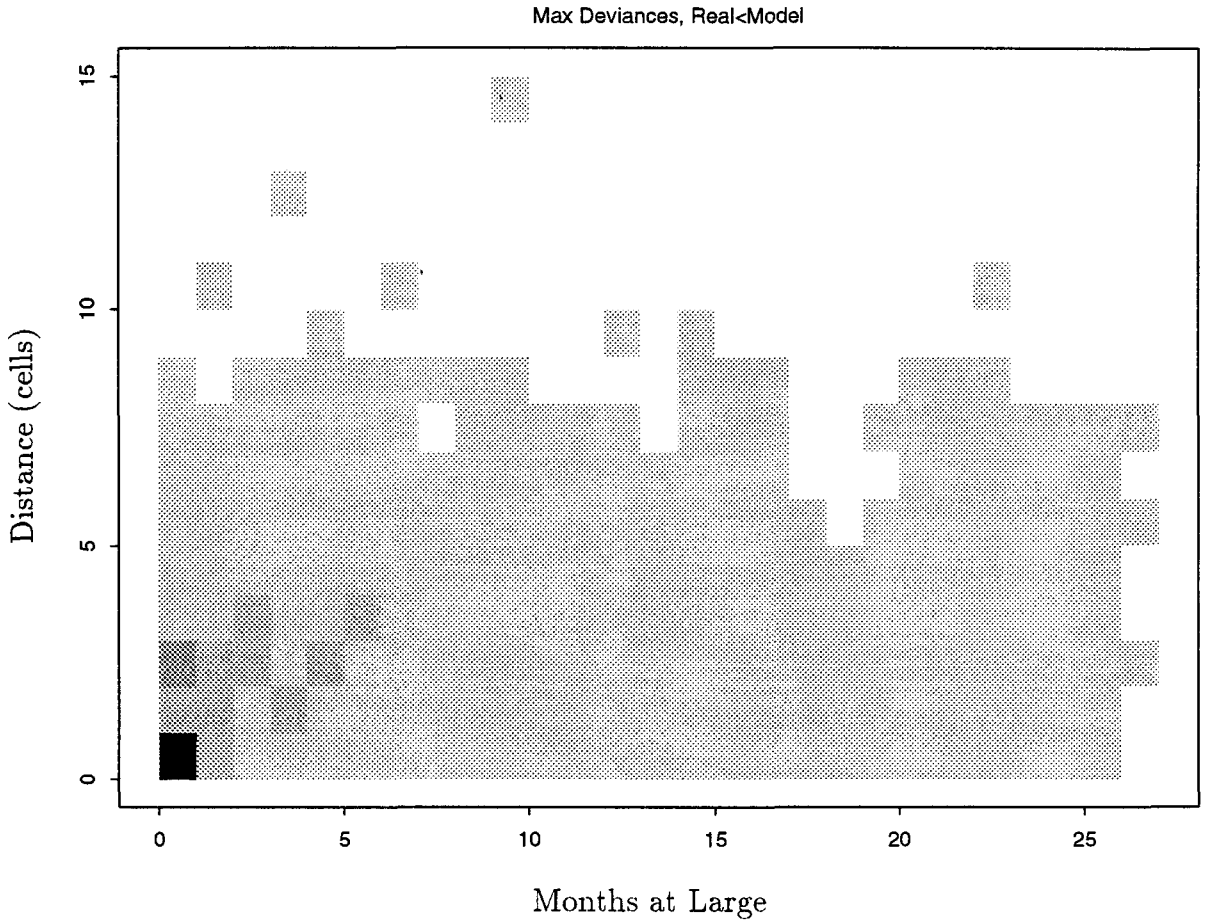

Figure 10. Maxima of deviances in categories of distance from cell of release (measured in cell widths of 30 nm) and months at large, and for spatiotemporal strata in which the best fitting outcome of the model predicts greater than the real number of returns.